



# Luminescent metallomesogens based on platinum complex containing triphenylene unit



Junwei Shi, Yafei Wang\*, Manjun Xiao, Ping Zhong, Yu Liu, Hua Tan, Meixiang Zhu, Weiguo Zhu\*

College of Chemistry, Key Lab of Environment-Friendly Chemistry and Application of the Ministry of Education, Xiangtan University, Xiangtan 411105, China

## ARTICLE INFO

### Article history:

Received 20 October 2014

Accepted 28 November 2014

Available online 3 December 2014

### Keywords:

Metallomesogens

Platinum complexes

Triphenylene

Donor–acceptor framework

Luminescence

## ABSTRACT

To explore the influence of mesogenic unit on the liquid crystals and luminescence properties of metal complex, two novel triphenylene-based platinum complexes of TppyPtacac and TppyPtPhacac featuring donor–acceptor framework have been designed and synthesized, in which Tppy is triphenylene–phenylpyridine skeleton and acac/Phacac is pentane-2,4-dione derivative. Differential scanning calorimetry (DSC), polarized optical microscopy (POM) and X-ray diffraction (XRD) techniques demonstrate the complex TppyPtPhacac shows a column mesophase in the region of 55–110 °C. Both platinum complexes exhibit intense emission at about 550 nm in CH<sub>2</sub>Cl<sub>2</sub> solution. Compared to the analogous platinum complexes without triphenylene unit, TppyPtacac and TppyPtPhacac display a remarkable red-shifted emission profiles (ca. 50 nm) due to strong intramolecular charge transfer. Furthermore, the hole mobilities up to  $2.5 \times 10^{-4} \text{ cm}^2 \text{ V}^{-1} \text{ s}^{-1}$  and  $2.99 \times 10^{-5} \text{ cm}^2 \text{ V}^{-1} \text{ s}^{-1}$  are achieved for the annealed film of TppyPtacac and TppyPtPhacac, respectively, which is one of the highest hole mobility with respect to cyclometalated platinum complexes.

© 2014 Elsevier Ltd. All rights reserved.

## 1. Introduction

Over the past two decades, luminescent liquid crystals (LC) materials have attracted much attention as charming candidates for organic optoelectronics devices, especially for polarized organic light-emitting diodes (OLEDs) owing to the combination of the optoelectronic characteristics of luminescent materials with the unique properties of anisotropic fluids.<sup>1–3</sup> To date, numerous efforts have been devoted to design luminescent LC materials based on small molecules,<sup>4,5</sup> polymers<sup>6,7</sup> and metal complexes.<sup>8,9</sup> Among these materials, the luminescent LC materials with metal ions (luminescent metallomesogens) are a particularly enticing family due to their outstanding optoelectrical and magnetic characteristics combined with the properties of anisotropic fluids.

To this end, platinum complexes are one of the most attractive candidates for luminescent metallomesogens due to the possibility of nearly 100% internal quantum efficiency, square-planar geometry, strong intermolecular Pt···Pt interaction and diverse charge transfer transition (e.g., metal-metal-to-ligand charge transfer, excimeric ligand-to-ligand charge transfer).<sup>10–13</sup> To the best of our

knowledge, most platinum-based luminescent metallomesogens employed nitrogen-containing heteroaromatic derivatives (2-phenylpyridine/2-phenylpyrimidines) as the cyclometalated ligands and acetylacetonate derivatives as the ancillary ligands.<sup>14–20</sup> Tschierske and co-workers prepared a series of platinum-based luminescent metallomesogens containing rod-like 2-phenylpyrimidines/2-phenylpyridines ligand. The effect of the molecular structure on the mesogens (lamellar, nematic and columnar phase) and luminescence properties were systematically investigated.<sup>14,15</sup> Subsequently, the functionalized bidentate and terdentate platinum complexes have received considerable attention in luminescent metallomesogens. Bruce et al. reported the half-disc *N,C,N*-Pt(II) complexes possessing a column mesogen and phase state-dependent emission spectra.<sup>16</sup> The rod-like, *ortho*-platinated complexes bearing 2,5-diphenylpyrimidines and β-diketone ligands showed a smectic phase and strong luminescence ( $\Phi_{\text{em}} > 50\%$ ), reported by the same group.<sup>17,18</sup> Recently, we also presented the luminescent metallomesogens based on mononuclear and dinuclear platinum complexes.<sup>19,20</sup> Both of the mono-/dinuclear platinum complexes possessed green emission in the smectic phase. However, all of these platinum-based luminescent metallomesogens are comprised of rigid cyclometalated ligand and peripheral flexible chains. Few investigations in the platinum complex with a pendant mesogens unit have been explored.<sup>21</sup>

\* Corresponding authors. Tel.: +86 731 58293377; fax: +86 731 58292251; e-mail addresses: [wangyf\\_miracle@hotmail.com](mailto:wangyf_miracle@hotmail.com) (Y. Wang), [zhuwg18@126.com](mailto:zhuwg18@126.com) (W. Zhu).

With this in mind, we focus our attention on the structure–property relationship in mesogenic unit and luminescent metallomesogens. Inspired by a wide application of triphenylene unit in discotic liquid crystals and emission materials,<sup>21,22</sup> it could be available to favour the liquid crystal and charge mobility by introducing the triphenylene derivative into luminescent metallomesogens. Furthermore, encouraged by our previous work on platinum-based metallomesogens,<sup>19,20</sup> we designed and synthesized two novel triphenylene-based platinum complexes featuring donor–acceptor (D–A) framework, so-called TppyPtPhacac and TppyPtacac, in which the Tppy is the triphenylene-phenylpyridine skeleton and Phacac/acac is the pentane-2,4-dione derivative (Chart 1). In these molecules, the triphenylene derivative acts as the donor (D) unit while the platinum segment is considered as the acceptor group (A). Both D–A platinum complexes are expected to promote the mesogens and tuning the emission via intramolecular interaction.

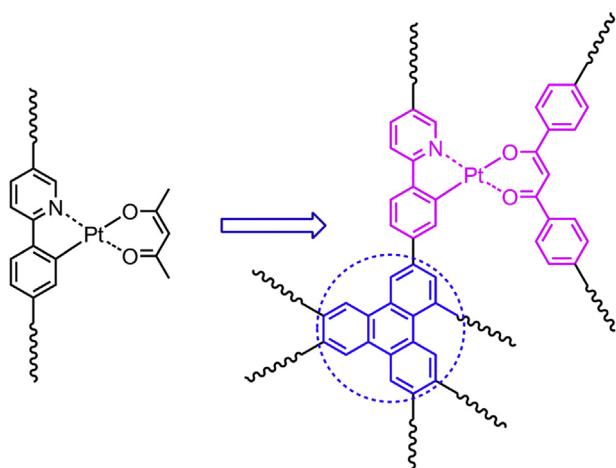


Chart 1. Structural evolution of platinum-based metallomesogens.

Herein, the preparation, liquid crystal and optophysical properties of both platinum complexes are discussed in detail. Complex TppyPtPhacac shows a column mesophase characterized by differential scanning calorimetry (DSC), polarized optical microscopy (POM) and X-ray diffraction (XRD) techniques. The hole mobilities up to  $2.5 \times 10^{-4} \text{ cm}^2 \text{ V}^{-1} \text{ s}^{-1}$  and  $2.99 \times 10^{-5} \text{ cm}^2 \text{ V}^{-1} \text{ s}^{-1}$  are achieved for the annealed film of TppyPtacac and TppyPtPhacac, respectively.

## 2. Results and discussion

### 2.1. Synthesis

The synthetic routes of platinum complexes are shown in Scheme 1. The key precursor triphenylene derivative **5** was prepared via a four-step reaction starting from pyrocatechol.<sup>24</sup> Then, compound **5** was reacted with **6**<sup>20</sup> to give the cyclometalated ligand **7** via Suzuki Coupling reaction in a moderate yield of 54.9%. Chloride-bridged dimer was obtained according to the previous procedure and used to the next step without any further purification.<sup>19</sup> Finally, cleavage reaction between chloride-bridged dimer and ancillary ligand (acac or **8**<sup>20</sup>) was carried out to afford the platinum complexes in 41–50% yield. The cyclometalated ligand and platinum complexes were characterized by <sup>1</sup>H NMR, <sup>13</sup>C NMR TOF-MS and elemental analysis.

### 2.2. Liquid crystalline properties

The thermal stability of these platinum complexes was evaluated by thermal gravity analysis (TGA). The decomposition temperatures with 5% weight loss are observed at 162 °C and 192 °C for TppyPtacac and TppyPtPhacac, respectively (Fig. S1). It is noted that TppyPtPhacac exhibits a better thermal stability owing to the additional phenyl units in the ancillary ligand.

On the other hand, the phase transition properties of TppyPtacac and TppyPtPhacac were characterized by DSC and POM. As shown in Fig. S2, only one endothermic peak at 152 °C is observed between the solid and isotropic phase while one exothermic transition at 118 °C is detected on the cooling circle. On contrary, the DSC curve of TppyPtPhacac shows two endothermic peaks at 55 °C and 110 °C, which are corresponding to the melting and clearing transitions. Notably, the melting point decreases with the increasing number of peripheral chains. However, only one peak at 50 °C is detected for TppyPtPhacac during the cooling scan, implying that an undetectable transition from isotropic to liquid crystal phase has occurred.<sup>21</sup>

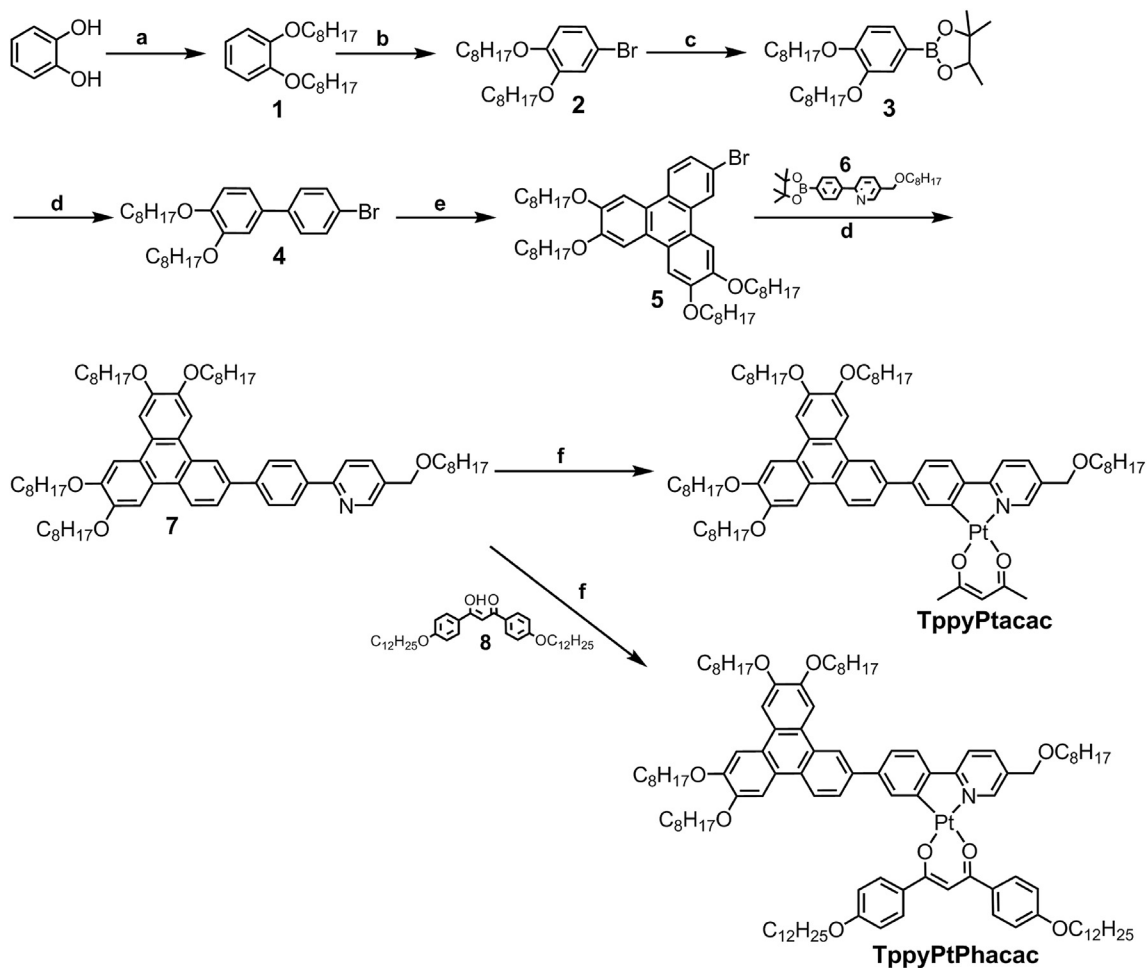
The POM study revealed that TppyPtacac presents a spherulitic texture (Fig. 1a) and no fluidity upon cooling circle, indicating that TppyPtacac could be a crystal. The complex of TppyPtPhacac exhibits a birefringent texture along with good fluidity during heating and cooling process. Even though no characteristic texture was observed, a distinct colour change from yellow to green is observed on heating process for TppyPtPhacac (Fig. 1b and c). According to these results, complex TppyPtPhacac is tentatively proved to be theomorphic LC property.

To further confirm the LC property, X-ray diffraction (XRD) was carried out for both platinum complexes. As in the case of TppyPtacac, the XRD diffraction pattern reveals a crystal packing with a disorder structure at 100 °C (Fig. S3). For TppyPtPhacac, as shown in Fig. 2, a distinct reflection peak at 17.9 Å and one weak peak at 15.7 Å, with a *d*-spacing ratio of 1/3<sup>1/2</sup>:2, are obtained, which demonstrates it is a column LC phase. Additionally, a diffuse peak in wide angle region (ca. 4.3 Å) is assigned to the loose ordering of the molten peripheral chains.<sup>25,26</sup> Compared to the previous work,<sup>19</sup> it is noted that the LC phase was changed from smectic to column via introducing the triphenylene derivative into platinum complex.

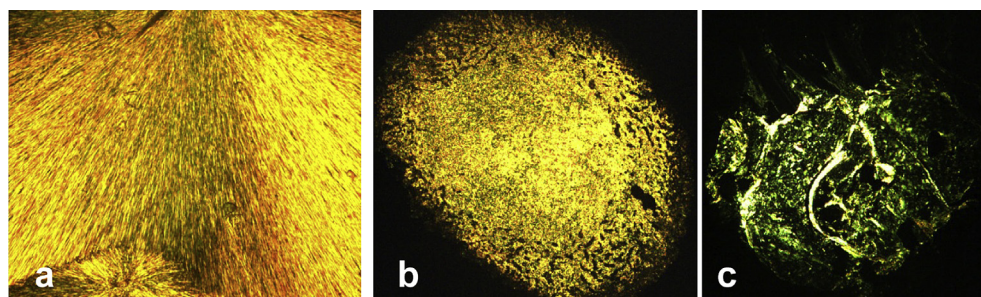
### 2.3. Optophysical properties

The UV–vis absorption and photoluminescent (PL) spectra of both platinum complexes were measured in CH<sub>2</sub>Cl<sub>2</sub> solution ( $10^{-5}$  M) and as a thin film at rt. As depicted in Fig. 3, similar absorption spectra are observed for both platinum complexes in the solution. The intense absorption bands in the region of 263–350 nm are attributed to the ligand centred <sup>1</sup>( $\pi$ – $\pi^*$ ) transitions.<sup>27</sup> The weak absorption bands from 360 nm to 474 nm are assigned to the metal-to-ligand charge transfer (MLCT) transition. Compared to the reported platinum complexes,<sup>19</sup> it implies that introducing the triphenylene unit into cyclometalated ligand has a strong effect on the absorption of platinum complexes.

Excitation with 450 nm at rt, both platinum complexes exhibit a maximum emission peak at about 550 nm ( $\pm 2$  nm) and a shoulder at about 592 nm. Compared to the reported 2-phenylpyridine-based metallomesogens,<sup>19</sup> TppyPtacac and TppyPtPhacac present a red-shifted emission (ca. 50 nm) in solution owing to an effective intramolecular charge transfer transition. The neat film of both platinum complexes display a remarkable bathochromic shifts (ca. 70 nm) with a maximum peak located at about 620 nm due to the formation of nonemission excimer or excimer-like adducts.<sup>21</sup> However, a monomer emission from TppyPtacac is observed in the neat film, which implies that the TppyPtPhacac has a more tendency to aggregation in the film.



Scheme 1. The synthetic route of platinum complexes.

Fig. 1. POM (100 $\times$ ) images: (a) TppyPtacac at  $120^\circ C$  on cooling circle; (b) TppyPtPhacac at room temperature; (c) TppyPtPhacac at  $70^\circ C$  on heating circle.

To gain insight into the influence of morphologies on PL emission, the temperature-dependent PL spectra of TppyPtPhacac were studied (Fig. 4a). A broad emission band at about 620 nm is presented. The emission peak and shape show a tiny change at different temperatures. It is noted that the emission intensity gradually decreases with increasing the temperature from  $28^\circ C$  to  $70^\circ C$ , which is attributed to the larger extent of self-quenching aggregates and increased thermally activated non-radioactive decay processes with increased temperature.<sup>26,28</sup> As described in

Fig. 4b, a dramatic decrease in emission intensity is presented in the crystal state, whereas the emission intensity displays the trend of stability in liquid crystal phase due to the well-organized structure.

#### 2.4. Hole mobilities

Charge mobility plays a vital role in organic optoelectronic materials. However, few investigations on the charge mobility of platinum complexes have been explored. Herein, the hole

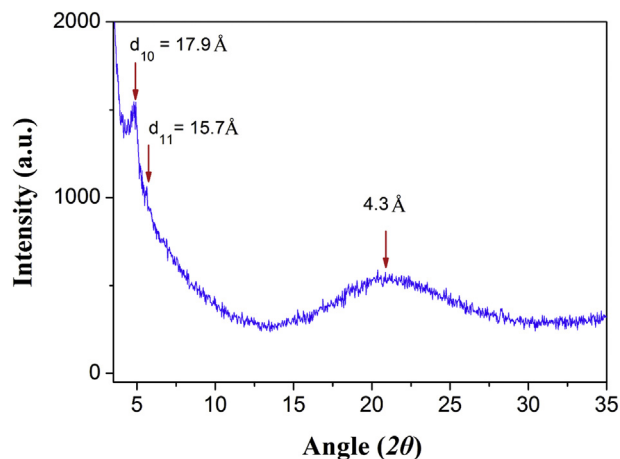


Fig. 2. XRD pattern of complex TppyPtPhacac at 80 °C.

mobilities of TppyPtacac and TppyPtPhacac were measured using space charge limited current (SCLC) model. The pristine films of TppyPtacac and TppyPtPhacac exhibit the hole mobilities of  $1.43 \times 10^{-5} \text{ cm}^2 \text{ V}^{-1} \text{ s}^{-1}$  and  $3.12 \times 10^{-6} \text{ cm}^2 \text{ V}^{-1} \text{ s}^{-1}$ , respectively. Upon thermal treatment at 100 °C for 30 min, the hole mobilities of TppyPtacac and TppyPtPhacac are  $2.5 \times 10^{-4} \text{ cm}^2 \text{ V}^{-1} \text{ s}^{-1}$  and  $2.99 \times 10^{-5} \text{ cm}^2 \text{ V}^{-1} \text{ s}^{-1}$ , respectively, which are higher than those of analogous platinum complexes.<sup>23,29</sup> Moreover, the hole mobilities of the annealed film are an order of magnitude higher than that of the pristine film. To further evaluate the affect of morphology on the hole mobility, the annealed film surface morphology of both platinum complexes was investigated by atomic force microscopic (AFM, Fig. 5). The AFM images reveal that the annealed neat films of TppyPtacac and TppyPtPhacac display small root-mean-square (rms) roughness of 1.45 nm and 0.50 nm, respectively. Obviously, the smooth surface of annealed film is responsible for an improved hole mobility.

### 3. Conclusions

Two novel D–A platinum-based luminescent metallomesogens bearing triphenylene unit were prepared and characterized. The TppyPtPhacac exhibited liquid crystal with column mesomorphism characterized by DSC, POM and XRD. Both platinum complexes revealed PL emission in the region of 500–600 nm. As expected, integrating the triphenylene derivative linkage together in platinum complex plays a positive role in favour of the liquid crystals property and effective intramolecular charge transfer. In addition, hole mobilities with the order of  $10^{-5}$ – $10^{-4}$  were achieved for the annealed films of platinum complexes. This research could provide a novel strategy for design the luminescent metallomesogens with D–A framework.

### 4. Experimental

#### 4.1. Materials and instrumentation

All reagents were purchased from Aldrich, J&K Chemical and Aladdin companies. All reactions were carried out under  $\text{N}_2$  atmosphere.  $^1\text{H}$  NMR and  $^{13}\text{C}$  NMR spectra were acquired using a Bruker Dex-400 NMR instrument using  $\text{CDCl}_3$  as a solvent. Mass spectra (MS) were recorded on a Bruker Autoflex MALDITOF instrument using dithranol as a matrix. The UV–vis absorption and photoluminescence spectra were measured with a Varian Cray 50

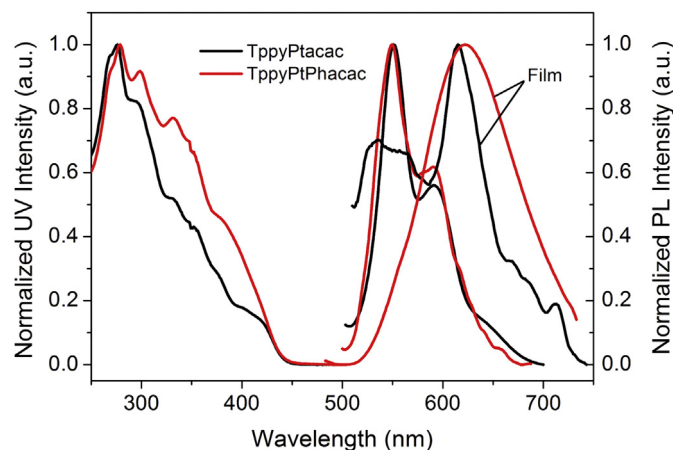


Fig. 3. Absorption spectra and PL spectra of platinum complexes in  $\text{CH}_2\text{Cl}_2$  and neat film at room temperature.

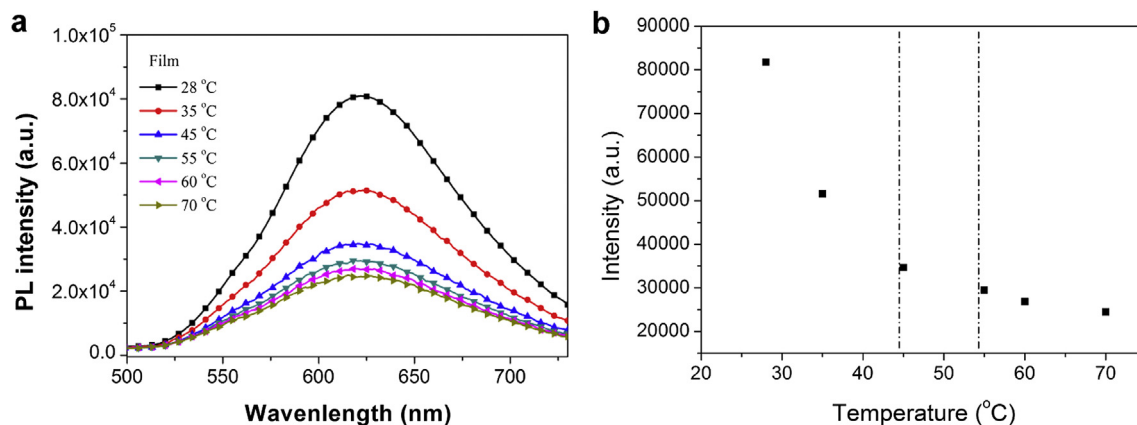
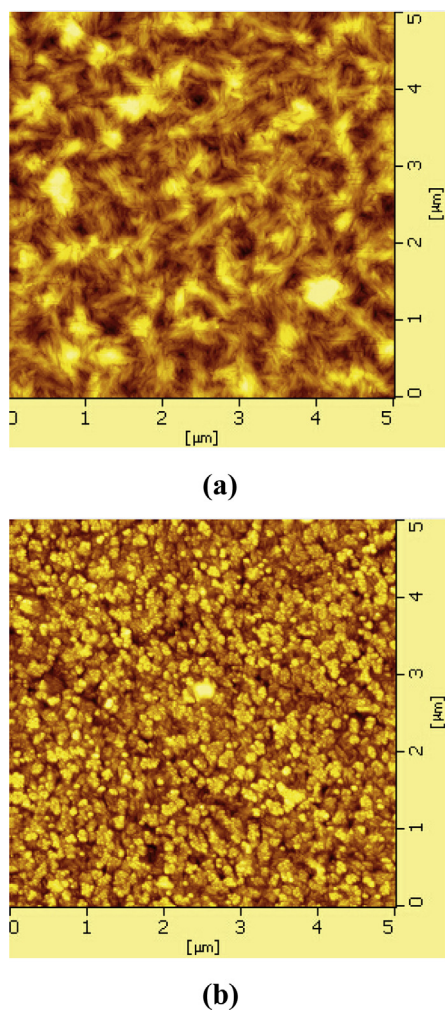


Fig. 4. (a) Temperature-dependence PL emission spectra of TppyPtPhacac complexes in thin film from 28 °C to 70 °C; (b) emission intensity of maximum wavelength versus temperature for TppyPtPhacac.



**Fig. 5.** AFM images of spin-coated films of (a) TppyPtacac, (b) TppyPtPhacac. The scanning area is  $5 \times 5 \mu\text{m}$  for all images.

and Perkin–Elmer LS50B luminescence spectrometer, respectively. TGA was carried out with an NETZSCH STA449 from  $25^\circ\text{C}$  to  $600^\circ\text{C}$  at a  $20^\circ\text{C}/\text{min}$  heating rate under  $\text{N}_2$  atmosphere. Differential scanning calorimetry (DSC) was measured the phase transition temperature with a rate of  $10^\circ\text{C}/\text{min}$  heating rate under  $\text{N}_2$  atmosphere. X-ray diffraction (XRD) with  $\text{Cu K}\alpha$  radiation ( $\lambda=1.5418 \text{ \AA}$ ) was measured the liquid crystal structure, and the scans were performed in continuous mode from  $1.5^\circ$  to  $35^\circ$  ( $2\theta$  angle).

## 4.2. Devices fabrication

The hole mobility was measured using the space charge limited current (SCLC) model with a devices configuration of ITO/PEDOT:PSS (40 nm)/Active Layer (100 nm)/ $\text{MoO}_3$  (10 nm)/Ag (100 nm). The active layer is the pristine film (or annealed film at  $100^\circ\text{C}$  for 30 min) of TppyPtacac and TppyPtPhacac. Indium tin oxide (ITO) was cleaned with the general procedures.<sup>23</sup> The PEDOT:PSS was spin-coated onto the ITO glass at 4000 rpm and then baked at  $160^\circ\text{C}$  for 15 min in air. The active layer was spin-cast from chloroform (20 mg/mL) at 1000 rpm for TppyPtacac and 2000 rpm for TppyPtPhacac. A  $\text{MoO}_3$  and Ag cathode was then thermally evaporated under vacuum ( $\sim 10^{-7}$  Torr) through a shadow mask defining an active device area of  $\sim 0.03 \text{ cm}^2$ . The hole mobilities were calculated according to the relative literature.<sup>23</sup>

## 4.3. 1,2-Bis(octyloxy)benzene (1)

A mixture of pyrocatechol (5.0 g, 45.5 mmol), 1-bromooctane (18.5 g, 96.0 mmol), potassium carbonate (25.0 g, 181.2 mmol), potassium iodide (0.5 g, 2.9 mmol) and tetrabutylammonium bromide (0.53 g, 1.64 mmol) was dissolved in ethanol (130 mL) and refluxed for 24 h under nitrogen atmosphere. After cooling to room temperature (rt), the reaction mixture was filtered and the solvent was removed by rotary evaporation. The residue was purified by silica gel column chromatography using petroleum ether (PE) as eluent to obtain oily liquid **1** (12.8 g, 84%).  $^1\text{H NMR}$  ( $\text{CDCl}_3$ , 400 MHz, TMS),  $\delta$  (ppm): 6.88 (s, 4H), 4.0 (t,  $J=6.0$  Hz, 4H), 1.84–1.77 (m, 4H), 1.46 (d,  $J=4.0$  Hz, 4H), 1.31–1.28 (m, 16H), 0.88 (t,  $J=8.0$  Hz, 6H).

## 4.4. 4-Bromine-1,2-bis(octyloxy)benzene (2)

To a stirred solution of compound **1** (1.0 g, 3.0 mmol) in THF (40 mL) was slowly added the mixture of *N*-bromosuccinimide (0.65 g, 3.7 mmol) and THF (10 mL) at  $0^\circ\text{C}$ . The reaction mixture was stirred for 8 h at  $0^\circ\text{C}$  in dark. Then the solvent was removed by rotary evaporation. The residue was purified by silica gel column chromatography using PE as eluent to give a yellow solid **2** (0.94 g, 78.3%).  $^1\text{H NMR}$  ( $\text{CDCl}_3$ , 400 MHz, TMS),  $\delta$  (ppm): 6.98 (d,  $J=4.0$  Hz, 2H), 6.73 (s, 1H), 3.95 (t,  $J=6.0$  Hz, 4H), 1.82–1.77 (m, 4H), 1.30–1.28 (m, 20H), 0.88–0.86 (m, 6H).

## 4.5. 2-(3,4-Bis(octyloxy)benzene)-4,4,5,5-tetramethyl-1,3,2-dioxaborolane (3)

A mixture of compound **2** (4.0 g, 9.68 mmol), bis(pinacolato)diboron (3.68 g, 15.4 mmol), potassium acetate (2.89 g, 29.0 mmol), and  $[1,1'\text{-bis}(\text{diphenyl-phosphino})\text{ferrocene}]\text{dichloropalladium(II)}$  (163 mg, 0.19 mmol) in 1,4-dioxane (120 mL) was reacted for 24 h at  $80^\circ\text{C}$  in nitrogen atmosphere. After cooling to rt, the reaction mixture was poured into water (50 mL) and extracted with  $\text{CH}_2\text{Cl}_2$  ( $3 \times 30$  mL). The combined organic layer was washed with water ( $3 \times 50$  mL) and dried with  $\text{Na}_2\text{SO}_4$ . The solvent was removed by rotary evaporation. Then, the crude product was purified by silica gel column chromatography using  $\text{PE}/\text{CH}_2\text{Cl}_2$  (v/v, 5:1) as eluent to give as oily solid **3** (2.13 g, 71%).  $^1\text{H NMR}$  ( $\text{CDCl}_3$ , 400 MHz, TMS),  $\delta$  (ppm): 7.39 (d,  $J=4.0$  Hz, 2H), 7.29 (s, 1H), 4.04–3.99 (m, 4H), 1.83–1.78 (m, 4H), 1.55–1.37 (m, 32H), 0.91–0.88 (m, 6H).

## 4.6. 1,2-Bis(octyloxy)-4(bromophenyl)benzene (4)

A mixture of compound **3** (5.0 g, 10.8 mmol), 4-bromiodobenzene (4.6 g, 16.3 mmol), tetrakis(triphenylphosphine)palladium(0) (374 mg, 0.324 mmol), and potassium carbonate (2 M, 20 mL) in THF (150 mL) was refluxed for 24 h under  $\text{N}_2$ . After cooling to rt, the reaction mixture was poured into water (50 mL) and extracted with  $\text{CH}_2\text{Cl}_2$  ( $3 \times 30$  mL). The combined organic layer was washed with water ( $3 \times 50$  mL) and dried with  $\text{Na}_2\text{SO}_4$ . The solvent was removed by rotary evaporation and the residue was purified by silica gel column chromatography using  $\text{PE}/\text{CH}_2\text{Cl}_2$  (v/v, 10:1) as eluent to give as a white solid **4** (2.8 g, 53.8%).  $^1\text{H NMR}$  ( $\text{CDCl}_3$ , 400 MHz, TMS),  $\delta$  (ppm): 7.52 (d,  $J=8.36$  Hz, 2H), 7.40 (d,  $J=9.57$  Hz, 2H), 7.07 (d,  $J=6.69$  Hz, 2H), 6.88 (s, 1H), 4.03 (t,  $J=6.7$  Hz, 4H), 1.85 (t,  $J=6.89$  Hz, 4H), 1.25–0.88 (m, 20H), 0.88–0.87 (m, 6H).

## 4.7. 10-Bromine-2,3,6,7-tetra(octyloxy)-benzophenanthrene (5)

To a stirred solution of compound **1** (1.4 g, 4.08 mmol) and compound **4** (1.0 g, 2.04 mmol) in  $\text{CH}_2\text{Cl}_2$  (50 mL) was added iron(III) chloride anhydrous (991 mg, 6.12 mmol). The reaction mixture was stirred for 0.5 h at rt and quenched with methanol. The mixture was poured into water (50 mL) was extracted with  $\text{CH}_2\text{Cl}_2$ .

The combined organic layer was washed with water and dried with  $\text{Na}_2\text{SO}_4$ . Then, the solvent was removed by rotary evaporator and the residue was purified by silica gel column chromatography using  $\text{PE}/\text{CH}_2\text{Cl}_2$  (v/v, 10:3) as eluent to give compound **5** as a solid (730 mg, 43.5%).  $^1\text{H}$  NMR ( $\text{CDCl}_3$ , 400 MHz, TMS),  $\delta$  (ppm): 8.56 (s, 1H), 8.31 (d,  $J=8.68$  Hz, 1H), 7.93–7.81 (m, 4H), 7.64 (d,  $J=8.64$  Hz, 1H), 4.24 (t,  $J=6.4$  Hz, 8H), 1.94–1.88 (m, 8H), 1.40–1.31 (m, 40H), 0.88–0.90 (m, 12H).

#### 4.8. 2-(4-(2,3,6,7-Tetraoctyloxybenzophenanthrene)phenyl)-5-((octyloxy)methyl)pyridine (7)

A mixture of compound **5** (678 mg, 0.827 mmol), compound **6** (350 mg, 0.827 mmol), tetrakis(triphenylphosphine)palladium(0) (38 mg, 0.033 mmol) and caesium carbonate (2 M, 10 mL) in toluene (40 mL) was heated to 80 °C for 24 h in  $\text{N}_2$  atmosphere. After cooling to rt, the reaction mixture was poured into water (50 mL) and extracted with  $\text{CH}_2\text{Cl}_2$ . The combined organic layer was washed with water and dried with  $\text{Na}_2\text{SO}_4$ . Then, the solvent was removed by rotary evaporator. The residue was purified by silica gel column chromatography using  $\text{CH}_2\text{Cl}_2/\text{PE}$  (v/v, 10:1) as eluent to give a yellow solid **10** (470 mg, 54.9%).  $^1\text{H}$  NMR ( $\text{CDCl}_3$ , 400 MHz, TMS),  $\delta$  (ppm): 8.68 (s, 1H), 8.55 (d,  $J=8.70$  Hz, 2H), 8.21 (s, 1H), 8.20–8.03 (m, 4H), 8.10 (d,  $J=8.03$  Hz, 2H), 7.90 (d,  $J=7.8$  Hz, 2H), 7.80 (s, 2H), 4.58 (s, 2H), 4.25 (t,  $J=6.31$  Hz, 8H), 3.53 (t,  $J=6.56$  Hz, 2H), 1.95 (t,  $J=6.60$  Hz, 8H), 1.41–1.25 (m, 52H), 0.90–0.88 (m, 15H).  $^{13}\text{C}$  NMR (100 MHz,  $\text{CDCl}_3$ ),  $\delta$  (ppm): 14.06, 22.65, 26.21, 29.34, 29.54, 31.84, 69.54, 69.73, 69.81, 70.12, 70.99, 107.45, 107.63, 120.29, 121.34, 123.54, 123.80, 124.39, 124.64, 125.03, 127.47, 127.77, 128.38, 129.27, 132.86, 136.68, 137.97, 142.25, 148.69, 149.27, 149.79, 149.87, 156.09. MALDI-MS ( $m/z$ ): 1035.735 for  $[\text{M}^+]$ .

#### 4.9. Synthesis of the complex TppyPtacac

To a mixture of  $\text{K}_2\text{PtCl}_4$  (18.2 mg, 0.044 mmol) and water (3 mL) was added a solution of compound **10** (100 mg, 0.096 mmol) in chloroform (8 mL) and 2-ethoxyethanol (3 mL). The reaction mixture was heated to 80 °C for 24 h in  $\text{N}_2$  atmosphere. After cooling to rt, the reaction mixture was extracted with  $\text{CH}_2\text{Cl}_2$  and washed with water. The organic layer was collected and dried with  $\text{Na}_2\text{SO}_4$ . After removing the solvent, the di- $\mu$ -chloro dimer was obtained and used to the next step without any further purification.

A mixture of di- $\mu$ -chloro dimer (680 mg, 0.269 mmol), pentane-2,4-dione (108 mg, 1.076 mmol), and sodium carbonate (285 mg, 2.69 mmol) in dry 2-ethoxyethanol (25 mL) was refluxed for 24 h in  $\text{N}_2$ . After cooling to rt, the mixture was poured into water (50 mL) and extracted with  $\text{CH}_2\text{Cl}_2$  (3  $\times$  30 mL). The combined organic layer was washed with water and dried with  $\text{Na}_2\text{SO}_4$ . After removing the solvent by rotary evaporation, the residue was passed through a flash silica gel column using  $\text{CH}_2\text{Cl}_2/\text{PE}$  (v/v, 2:1) as the eluent to give a yellow solid (120 mg, yield 33.5%).  $^1\text{H}$  NMR ( $\text{CDCl}_3$ , 400 MHz, TMS),  $\delta$  (ppm): 8.99 (s, 1H), 8.76 (s, 1H), 8.55 (d,  $J=4.3$  Hz, 1H), 8.12 (s, 1H), 8.04 (d,  $J=3.05$  Hz, 2H), 7.92 (d,  $J=4.13$  Hz, 2H), 7.85 (d,  $J=4.46$  Hz, 2H), 7.67 (dd, 1H), 7.59 (dd, 1H), 7.53 (dd, 1H), 5.51 (s, 1H), 4.59 (s, 2H), 4.26 (t,  $J=6.5$  Hz, 8H), 3.55 (t,  $J=6.49$  Hz, 2H), 2.03 (d,  $J=4.06$  Hz, 8H), 1.69–1.23 (m, 58H), 0.90–0.88 (m, 15H).  $^{13}\text{C}$  NMR (100 MHz,  $\text{CDCl}_3$ ),  $\delta$  (ppm): 14.19, 22.70, 26.24, 27.24, 28.29, 29.27, 29.36, 29.47, 29.52, 29.55, 29.71, 29.77, 31.88, 69.46, 69.63, 69.83, 71.12, 102.50, 109.49, 118.08, 121.49, 123.03, 123.23, 123.31, 123.81, 124.27, 125.55, 128.17, 129.15, 132.46, 137.33, 139.39, 142.00, 143.85, 146.15, 149.23, 149.27, 149.67, 167.13, 184.05, 185.83. MALDI-MS ( $m/z$ ): 1329.035 for  $[\text{M}^+]$ . Anal. Calcd for  $\text{C}_{75}\text{H}_{107}\text{NO}_7\text{Pt}$ : C, 67.74; H, 8.11; N, 1.05. Found: C, 67.02; H, 8.20; N, 1.02.

#### 4.10. Synthesis of the complex TppyPtPhacac

Complex TppyPtPhacac was prepared similarly to complexes TppyPtacac, using di- $\mu$ -chloro dimer (312 mg, 0.123 mmol), compound **8** (180 mg, 0.308 mmol), sodium carbonate (130 mg, 1.23 mmol) and dry 2-ethoxyethanol (20 mL). TppyPtPhacac was obtained as a yellow solid (90 mg, yield 37.6%).  $^1\text{H}$  NMR ( $\text{CDCl}_3$ , 400 MHz, TMS),  $\delta$  (ppm): 9.25 (s, 1H), 8.95 (s, 1H), 8.61 (d,  $J=4.3$  Hz, 1H), 8.37 (s, 1H), 8.17 (d,  $J=4.59$  Hz, 3H), 8.11 (d,  $J=4.40$  Hz, 2H), 7.96–7.82 (m, 5H), 7.73 (d,  $J=8.0$  Hz, 1H), 7.64 (d,  $J=8.1$  Hz, 1H), 7.61 (d,  $J=7.8$  Hz, 1H), 7.01 (d,  $J=4.34$  Hz, 2H), 6.82 (t,  $J=8.75$  Hz, 2H), 6.79 (s, 1H), 4.66 (s, 2H), 4.33–4.26 (s, 6H), 4.06 (t,  $J=6.4$  Hz, 2H), 3.9 (t,  $J=2.96$  Hz, 2H), 3.80 (t,  $J=3.0$  Hz, 2H), 3.63 (t,  $J=6.5$  Hz, 2H), 2.0 (t,  $J=3.45$  Hz, 7H), 1.86 (t,  $J=3.4$  Hz, 3H), 1.74 (t,  $J=3.42$  Hz, 8H), 1.36–1.14 (m, 82H), 0.94–0.90 (m, 21H).  $^{13}\text{C}$  NMR (100 MHz,  $\text{CDCl}_3$ ),  $\delta$  (ppm): 14.09, 22.71, 26.23, 26.26, 26.27, 26.29, 29.31, 29.38, 29.47, 29.53, 29.60, 29.68, 29.72, 31.84, 31.87, 31.90, 31.95, 67.85, 68.18, 69.16, 69.57, 69.79, 69.88, 71.28, 95.27, 106.76, 107.07, 114.29, 121.63, 123.31, 124.22, 124.27, 124.38, 125.40, 128.18, 128.70, 128.82, 129.42, 132.99, 126.87, 139.62, 146.20, 149.43, 149.58, 149.70, 161.45, 167.04, 178.62. MALDI-MS ( $m/z$ ): 1821.315 for  $[\text{M}^+]$ . Anal. Calcd for  $\text{C}_{109}\text{H}_{159}\text{NO}_9\text{Pt}$ : C, 71.83; H, 8.79; N, 0.77. Found: C, 71.79; H, 8.83; N, 0.72.

#### Acknowledgements

Financial support from the National Natural Science Foundation of China (21202139, 51273168 and 21172187), the Innovation Group in Hunan Natural Science Foundation (12JJ7002), The Scientific Research Fund of Hunan Provincial Education Department (12B123), Natural Science Foundation of Hunan (12JJ4019, 11JJ3061).

#### Supplementary data

Supplementary data associated with this article can be found in the online version, at <http://dx.doi.org/10.1016/j.tet.2014.11.070>.

#### References and notes

- Dyreklev, P.; Berggren, M.; Inganäs, O.; Andersson, M. R.; Wennerström, O.; Hjertberg, T. *Adv. Mater.* **1995**, *7*, 43–45.
- Lin, M. Y.; Chen, H. H.; Hsu, K. H.; Huang, Y. H.; Chen, Y. J.; Lin, H. Y.; Wu, Y. K. *IEEE Photon. Tech. L.* **2013**, *25*, 1321–1323.
- Liedtke, A.; O'Neill, M.; Wertmoller, A.; Kitney, S. P.; Kelly, S. M. *Chem. Mater.* **2008**, *20*, 3579–3586.
- Yasuda, T.; Ooi, H.; Morita, J.; Alama, Y.; Minoura, K.; Funahashi, M.; Shimomura, T.; Kato, T. *Adv. Funct. Mater.* **2009**, *19*, 411–419.
- Han, J. J. *Mater. Chem. C* **2013**, *1*, 7779–7797.
- Grell, M.; Bradley, D. D. C. *Adv. Mater.* **1999**, *11*, 895–905.
- Grell, M.; Knoll, W.; Lupo, D.; Meisel, A.; Miteva, T.; Neher, D.; Nothofer, H.; Scherf, U.; Yasuda, A. *Adv. Mater.* **1999**, *11*, 671–675.
- Binnemans, K. J. *Mater. Chem.* **2009**, *19*, 448–453.
- Blight, B. A.; Ko, S. B.; Lu, J. S.; Smith, L. F.; Wang, S. *Dalton Trans.* **2013**, *42*, 10089–10092.
- Fan, C.; Yang, L. C. *Chem. Soc. Rev.* **2014**, *43*, 6439–6469.
- Zhou, G. J.; Wong, W. Y. *Chem. Soc. Rev.* **2011**, *40*, 2541–2566.
- Kalinowski, J.; Fattori, V.; Cocchi, M.; Williams, J. A. G. *Coord. Chem. Rev.* **2011**, *255*, 2401–2425.
- Rausch, F.; Homeier, H. H. H.; Yersin, H. *Top. Organomet. Chem.* **2010**, *29*, 193–235.
- Hegmann, T.; Kain, J.; Diele, S.; Schubert, B.; Bögel, H.; Tschierske, C. *J. Mater. Chem.* **2003**, *13*, 991–1003.
- Damm, C.; Israel, G.; Hegmann, T.; Tschierske, C. *J. Mater. Chem.* **2006**, *16*, 1808–1816.
- Kozhevnikov, V.; Donnio, B.; Bruce, D. W. *Angew. Chem., Int. Ed.* **2008**, *47*, 6286–6289.
- Santoro, A.; Whitwood, A. C.; Williams, J. A. G.; Kozhevnikov, V. G.; Bruce, D. W. *Chem. Mater.* **2009**, *21*, 3871–3882.
- Spencer, M.; Santoro, A.; Freeman, G.; Diez, A.; Murry, P. R.; Torroba, J.; Whitwood, A. C.; Yellowlees, L. J.; Williams, J. A. G.; Bruce, D. W. *Dalton Trans.* **2012**, *41*, 14244–14256.
- Wang, Y.; Liu, Y.; Luo, J.; Qi, H.; Li, X.; Ni, M.; Liu, M.; Shi, D.; Zhu, W.; Cao, Y. *Dalton Trans.* **2011**, *40*, 5046–5051.

20. Wang, Y.; Chen, Q.; Li, Y.; Liu, Y.; Tan, H.; Yu, J.; Zhu, M.; Wu, H.; Zhu, W.; Cao, Y. *J. Phys. Chem. C* **2012**, *116*, 5908–5914.
21. Tritto, E.; Chico, R.; Sanz-Enguita, G.; Folcia, C.; Ortega, J.; Coco, S.; Espinet, P. *Inorg. Chem.* **2014**, *53*, 3449–3455.
22. Krause, C.; Zorn, R.; Emmerling, F.; Falkenhagen, J.; Frick, B.; Huberd, P.; Schönhals, A. *Phys. Chem. Chem. Phys.* **2014**, *16*, 7324–7333.
23. Clem, T. A.; Kavulak, D. F. J.; Westling, E. J.; Fréchet, J. M. J. *Chem. Mater.* **2010**, *22*, 1977–1987.
24. Chen, H. M.; Zhao, K. Q.; Wang, L.; Hu, P.; Wang, B. Q. *Soft Mater.* **2011**, *9*, 359–381.
25. Krikorian, M.; Liu, S.; Swager, T. M. *J. Am. Chem. Soc.* **2014**, *136*, 2952–2955.
26. Giroto, E.; Eccher, J.; Vieira, A. A.; Bechtold, I. H.; Gallardo, H. *Tetrahedron* **2014**, *70*, 3355–3360.
27. Frey, J.; Curchod, B. F.; Scopelliti, R.; Tavernelli, I.; Rothlisberger, U.; Nazeeruddin, M. K.; Baranoff, E. *Dalton Trans.* **2014**, *43*, 5667–5679.
28. Tuzimoto, P.; Santos, D. M. P. O.; Moreira, T. D. S.; Cristiano, R.; Bechtold, I. H.; Gallardo, H. *Liq. Cryst.* **2014**, *41*, 1097–1108.
29. Zhao, X.; Piliago, C.; Kim, B.; Poulsen, D. A.; Ma, B.; Unruh, D. A.; Fréchet, J. M. J. *Chem. Mater.* **2010**, *22*, 2325–2332.